

# Comparison and analysis of Bearingless Permanent Magnet Synchronous Motor with different Magnetized Rotor

Tao Zhang<sup>1,2</sup>, Xinfeng Liu<sup>1</sup>, Lihong Mo<sup>1</sup>, Wei Ni<sup>1</sup>, Wei Hong Ding<sup>1</sup>, Juang Huang<sup>3</sup>, Xue Wang<sup>3</sup>

<sup>1</sup> Faculty of Automation, Huaiyin Institute of Technology, Huai'an 223005, China

<sup>2</sup> Jiangsu Engineering Research Center on Meteorological Energy Using and Control, Nanjing University of Information Science and Technology, Nanjing 210044, China

<sup>3</sup> School of Electrical and Information Engineering, Jiangsu University, Zhenjiang 212013, China

In this paper, a novel bearingless permanent magnet synchronous motor (BPMSM) is presented and researched which the Halbach magnetized permanent magnet rotor is adopted. First, producing mechanisms of radial suspension force and torque of BPMSM is analyzed. The mathematical models of radial suspension force and torque are deduced. Then, the air-gap magnetic field, back electromotive force (EMF), radial suspension force, and torque of BPMSM with Halbach magnetized rotor and radial magnetized rotor are calculated and compared. Finally, the prototype motor equipped with Halbach magnetized rotor is constructed. The experimental results are tested to verify the correctness and effectiveness of the presented novel motor.

**Index Terms**—Bearingless permanent magnet synchronous motor, Halbach magnetization, permanent magnet motor, finite element analysis, transient analysis.

## I. INTRODUCTION

BEARINGLESS PERMANENT magnet synchronous motor (BPMSM) has attracted considerable interests because of small size and lightweight, high power factor and high efficiency, and no need excitation current. However, at present, air gap magnetic field and back-EMF of BPMSM researched throughout the world are all the rectangular waves. Thus, the high order harmonics of air-gap magnetic field can result in large torque ripples, radial suspension force ripples and the rotor eddy current losses[1]. Furthermore, there is a tradeoff between permanent magnet thickness (and, hence, torque density) and radial suspension force generation. Halbach permanent magnet arrays offer many attractive features which can be effectively used in the design of the BPMSM. One of the important characteristics is that it can cancel the flux on one side of the array and strengthen the flux on the other side[2]. Therefore, permanent magnets essentially do not require any back iron, and the rotor structure can be hollow or nonmagnetic with very low rotational inertia. Furthermore, the distribution of air-gap magnetic field is sinusoidal. Therefore, they are ideal for the BPMSM applications, where high torque density and radial suspension force density, low torque ripples and radial suspension force ripples, sinusoidal back-EMF, and sinusoidal air-gap magnetic field are desired. In this paper, BPMSMs with different magnetized rotor are designed and analyzed. Based on detailed analysis of suspension control mechanism, the mathematical models of radial suspension force are introduced. Using finite element method, the air-gap field distributions, back-EMF, radial suspension force, and torque of BPMSM with Halbach magnetized rotor and radial magnetized rotor are calculated and compared. The prototype motor equipped with Halbach magnetized rotor is constructed. The rotor radial displacement and rotor trajectory are tested to verify the correctness and effectiveness of the presented novel BPMSM.

## II. ROTOR TOPOLOGIES

For a fair comparison, two rotor topologies are designed at the same stator, turns of torque winding and suspension winding, thickness of permanent magnet, electric loading, dimensions including the outer diameter of rotor and stack length. In Fig.1(a), rotor permanent magnet ring is composed of four magnets, and each magnet adopts radial magnetized mode. But in Fig.1(b), the magnet ring consists of twenty-four little magnets, and the Halbach magnetized mode is chosen to optimize the performances of the motor. The electromagnetic performances are calculated with 2D time-stepping finite element method (FEM).

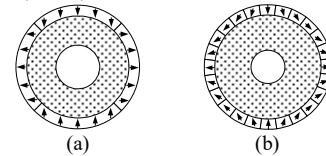


Fig. 1. Structure of permanent magnet rotor. (a) radial magnetization, (b) Halbach magnetization.

## III. FINITE ELEMENT ANALYSIS

### A. Air-gap magnetic field

Air-gap magnetic flux density data are extracted from the finite element models. In Fig.2(a), the air-gap magnetic flux density waveform is close to the rectangular wave with rich high order harmonics, and its fundamental amplitude is approximately equal to 0.7T. But in Fig.2(b), the waveform of air-gap magnetic flux density is a sine wave with less high harmonic contents, and its fundamental amplitude reaches to 0.9T.

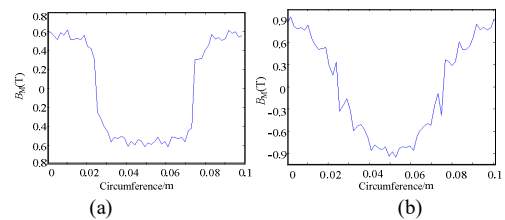


Fig.2 Air gap magnetic field waveform. (a) radial magnetization, (b) halbach array magnetization.

### B. No-load back EMF

The frequencies of suspension winding current and torque winding currents are set to 200Hz, 100Hz, respectively. The current amplitude is 5A; The initial phase difference  $\theta$  is equal to  $-135^\circ$ . The rotating mechanical angular velocity of the rotor is set to 30 00r/min, and the computation time is given from 0s to 0.2s. The time step size is configured to 0.001s. The no-load back-EMF waveforms are analyzed when the rotor is rotating in the geometric center position. It can be seen that the back-EMF frequency of torque windings are equal to 100Hz. In Fig.3(a), the amplitude of back-EMF waveforms is 133V. But in Fig.3(b), the amplitude of back-EMF waveforms is 142V for the larger air-gap flux density. Moreover, the back-EMF waveform of the motor with Halbach magnetized rotor is much more sinusoidal than the motor with the radial magnetized rotor.

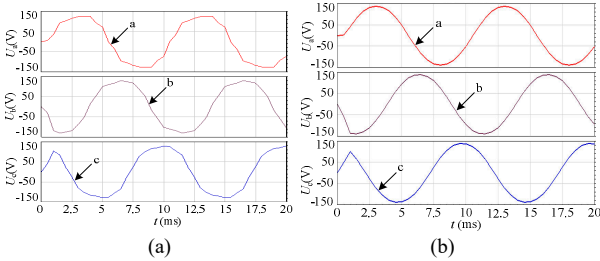


Fig.3. Back-EMF waveforms of torque windings, (a) radial magnetization, (b) Halbach magnetization.

### C. Radial suspension force

The transient radial suspension force waveforms are calculated. It can be seen that the force  $F_x$  is always equal to negative  $F_y$  because the direction of resultant radial suspension force is always pointed to the angle  $\theta$ . The resultant radial suspension force waveform is fluctuant from 280N to 300N, as shown in Fig.4(a), and its average value is equal to 287N. In Fig.4(b), the radial suspension force is approximately equal to 300N, and suspension force per unit current is equal to 60N. Moreover, the radial suspension force ripples of the motor with radial magnetized rotor are much larger than that with Halbach magnetized rotor.

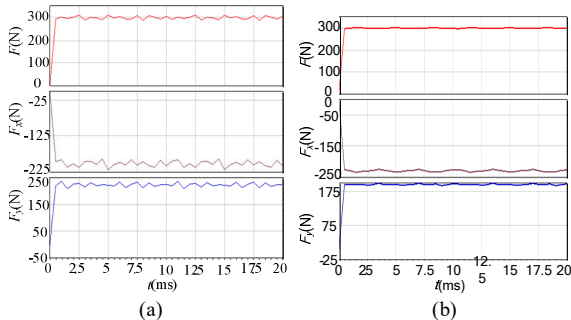


Fig.4. Radial suspension force waveforms. (a) radial magnetization, (b) Halbach magnetization.

### D. Torque

The transient torques are compared. The torque amplitude, in Fig.5(a), is approximately equal to 2.87Nm, but that in Fig.5(b) is equal to 3.3Nm, which is 15% larger than the

former one for the large air-gap magnetic flux density. Moreover, the torque ripples in Fig.5(b) is significantly bigger than that in Fig.5(a).

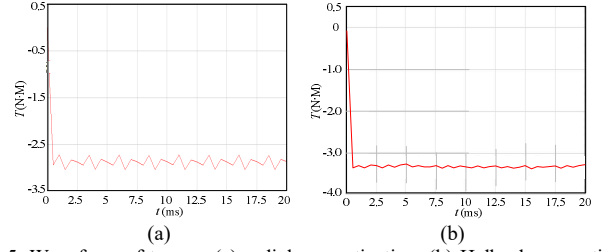
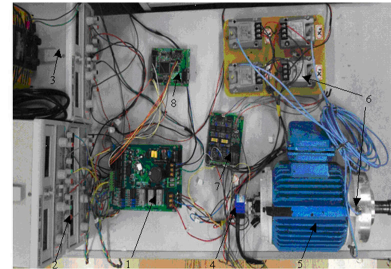


Fig.5. Waveform of torque. (a) radial magnetization, (b) Halbach magnetization.

## IV. EXPERIMENTS AND CONCLUSIONS

To verify the effectiveness of the proposed BPMSM with Halbach magnetized rotor, and theoretical analysis, a two degrees of freedom experimental prototype motor and platform, as shown in Fig.6(a), are made and tested. Fig.6(b) shows the radial displacements in x- and y-direction, and Fig.6(c) gives the rotor trajectory diagram. From the experimental results, the BPMSM proposed in this paper can rotate and suspend the rotor stably, and the vibration amplitude of the rotor radial displacement is about  $25\mu\text{m}$ . From the comparisons of the results from FEA simulation, we can see the merits of BPMSM with Halbach magnetized rotor which is helpful for BPMSM design and performance optimization.



1.inverter, 2.direct current power supply, 3. alternating current power supply, 4.rotary encoder, 5.BPMSM, 6. displacement sensor, 7. interface circuit, 8.controller.

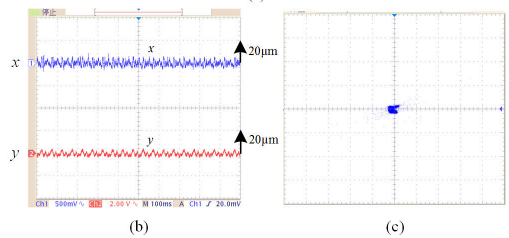


Fig.6. Experimental prototype BPMSM (a); radial displacements in x and y direction (b); rotor trajectory diagram (c).

## REFERENCES

- [1] S. Xiaodong, C. Long, Y. Zebin. "Overview of bearingless permanent magnet synchronous motor," IEEE Transactions on industrial electronics, 2013, Vol. 60, No. 12, pp. 5528-5538.
- [2] S. Dwari, L. Parsa. "Design of Halbach-array-based permanent-magnet motors with high acceleration," IEEE Transactions on Industrial Electronics, 2011, Vol.58, No.9, pp. 3768-3775.